Planar analysis of a quasi-zero stiffness mechanism using inclined linear springs

William S. P. Robertson, Ben Cazzolato, and Anthony Zander

School of Mechanical Engineering, The University of Adelaide, Australia

ABSTRACT

Negative stiffness mechanisms have seen renewed attention in recent years for their ability to reduce the resonance frequency of a structure without impeding their load-bearing ability. Such systems are often described as having quasi-zero stiffness when the negative stiffness is tuned to reduce the overall stiffness of the system as close to zero as possible without creating an instability. The system analysed in this work consists of a vertical spring for load bearing, and two symmetric inclined springs which behave with a snap-through effect to achieve negative stiffness. While this structure has been analysed extensively in the literature, generally only the stiffness in the vertical direction has been considered in the past. Here, the horizontal stiffness is assessed as well, and it is shown that it is possible to achieve quasi-zero stiffness in both directions simultaneously if the spring stiffnesses and pre-loads are chosen sufficiently. Attention is paid to the tuning required in order to set the equilibrium point at a position which is arbitrarily close to having quasi-zero stiffness while avoiding issues arising from mechanical instability.

INTRODUCTION

In recent years a number of nonlinear systems have been proposed for vibration isolation to overcome the trade-off between low stiffness and high load bearing. These systems in general use a combination of positive and negative stiffness elements to achieve a localised region of 'quasi–zero stiffness' at or near the equilibrium position of the system (Xing, Xiong, and Price 2005).

One system that exemplifies this idea involves using a repelling magnet pair to provide load bearing and an attracting magnet pair to provide negative stiffness (Robertson, Kidner, Cazzolato, and Zander 2009; Zhu, Cazzolato, Robertson, and Zander 2011), which has been investigated previously by the authors. The noncontact forces of the magnetic system make them well-suited for online tuning (Zhou and Liu 2010; Xu, Yu, Zhou, and Bishop 2013), but the inherent instability of magnetic systems can add complexity to the control required.

While flexible structures have been shown to operate in a similar manner (Tarnai 2003; Cella, Sannibale, DeSalvo, Marka, and Takamori 2005; Lee, Goverdovskiy, and Temnikov 2007), the most commonly investigated structure for achieving quasi–zero stiffness involves arrangements of inclined mechanical springs which generally operate in 'buckling' regimes such as the spring arrangement shown in Figure 1 (Molyneux 1957; Alabuzhev, Gritchin, Kim, Migirenko, Chon, and Stepanov 1989; Carrella, Brennan, and Waters 2007; Carrella, Brennan, Kovacic, and Waters 2009). This system consists of a load bearing vertical spring in parallel with a pair of inclined springs that behave in a buckling regime. Generally, analyses of this system have only considered its stiffness properties in a single degree of freedom, in the direction of the primary load bearing.

This paper consists of an analysis of the quasi-static behaviour of this inclined spring system and re-formulates the force and stiffness characteristics in both vertical and horizontal directions, describing in some detail the approach by which low stiffness in both directions can be achieved. Low stiffness in the vertical direction has been previously documented (as cited previously) due to the negative vertical stiffness of a pair of horizontal springs in compression. Low stiffness in the horizontal direction is newly analysed here, which is achieved due to the negative stiffness in the horizontal direction of the load-bearing vertical spring.

GEOMETRY

Figure 1a shows the planar inclined spring system without load
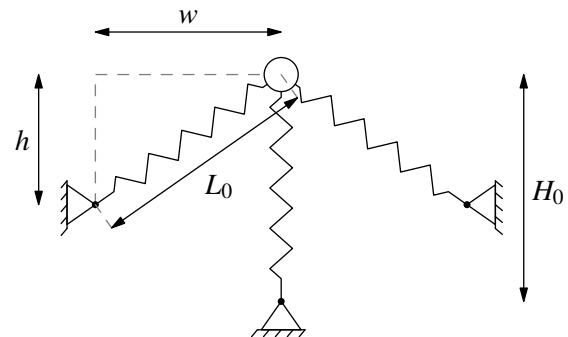
(a) Inclined springs in their uncompressed state, corresponding to a vertical displacement of $z = h$.
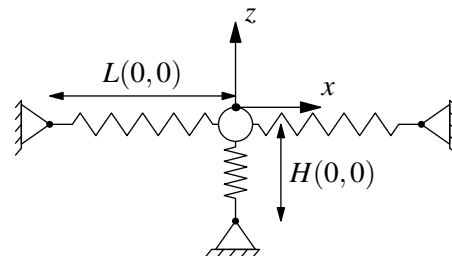
(b) Inclined springs at a position of maximum negative stiffness, corresponding to a vertical displacement of $z = 0$.

Figure 1. Negative stiffness inclined springs in parallel with a positive stiffness spring.

(that is, with undeflected springs) and Figure 1b shows the same system after deflection to the position which has the potential of achieving 'quasi–zero stiffness', which is the position of maximum compression of the inclined springs. The overall stiffness of the system must be tuned to support the mass of the load at this position.

At the unloaded state shown in Figure 1a, all springs are considered to be in their uncompressed state; with inclined spring lengths $L_0 = \sqrt{h^2 + w^2}$ and vertical spring length $H_0 = \eta L_0$, where η is denoted the 'length ratio' between the vertical and inclined springs. The inclined springs each have stiffness k_i and the vertical spring has stiffness $k_v = \alpha k_i$, with α denoted the 'stiffness ratio' between the vertical and inclined springs. The stiffness and deflection properties of the springs are summarised in Table 1.

Table 1. Properties of the springs in the quasi–zero stiffness inclined spring system defining stiffness ratio α and length ratio η.

Spring	Stiffness	Undeflected length
Inclined	k_i	$L_0 = \sqrt{h^2 + w^2}$
Vertical	$k_v = \alpha k_i$	$H_0 = \eta L_0$

The position of maximum compression of the inclined spring, shown in Figure 1b, defines the displacement origin of the system, where z is the displacement in the load bearing direction, and x is the displacement in the non–load bearing direction (this is used later for the derivation of the horizontal stiffness of the system).

The deflected lengths of the springs from displacement (z,x) are $L(z,x)$ for the inclined spring and $H(z,x)$ for the vertical spring. The compressed length of the inclined spring (on the left) is

$$L(z,x) = \sqrt{x^2 + [w+y]^2}, \tag{1}$$

and the vertical spring length is

$$H(z,x) = \sqrt{x^2 + [z - h + H_0]^2}; \tag{2}$$

note that $L(h,0) = L_0$ and $H(h,0) = H_0$.

The geometry that has been chosen uses linear springs that are all arranged to be undeflected in the unloaded state of the system. Kovacic, Brennan, and Waters (2008) have explored the effects of including pretension and the use of nonlinear softening springs for vertical vibration isolation.

VERTICAL FORCES

The forces on the mass are calculated by looking at the components of the forces due to each spring individually. The force due to the inclined spring (on the left of Figure 1a), in the direction of the spring, is given by

$$F_i(z,x) = [L_0 - L(z,x)] k_i = \left[\sqrt{h^2 + w^2} - \sqrt{x^2 + [w+y]^2} \right] k_i. \tag{3}$$

Assuming only vertical displacement ($x = 0$), the vertical component of this inclined spring force is

$$F_{i_v}(z) = F_i(z,0) \frac{x}{L(z,0)} = z k_i \left[\frac{\sqrt{h^2 + w^2}}{\sqrt{w^2 + z^2}} - 1 \right]. \tag{4}$$

It is convenient to normalise this result by representing the lengths and displacements as ratios of the uncompressed height of the inclined springs. With the coordinate substitutions $\xi = z/h$ and $\gamma = w/h$, the inclined spring force in the vertical direction can be written in non-dimensional form as

$$\frac{F_{i_v}(\xi)}{hk_i} = \xi \left[\sqrt{\frac{\gamma^2 + 1}{\gamma^2 + \xi^2}} - 1 \right], \tag{5}$$

where γ is denoted the 'geometric ratio' of the system and ξ the normalised displacement.

This is a different normalisation than used in the literature (Carrella, Brennan, and Waters 2007; Carrella, Brennan, Kovacic, and Waters 2009); note that here $\gamma = 0$ corresponds to unloaded inclined springs at 90° (that is, vertical) before compression, and $\gamma = \infty$ corresponds to unloaded inclined springs at 0° (that is, horizontal). In the coordinate system used here, the displacement origin $z = 0$ corresponds to the position of maximum

compression of the inclined springs; that is, when they are horizontal.

Figure 2a illustrates the force characteristic of Eq. (5) versus normalised displacement for a range of geometric ratios γ. The 'snap-through' forces that cause the negative stiffness are especially strong for smaller values of geometric ratio γ (that is, the more vertical the spring angles before deflection in Figure 1a).
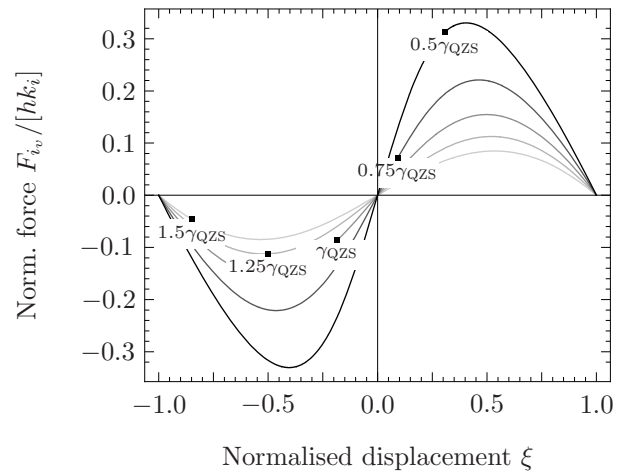
(a) Vertical force due to inclined springs only using Eq. (4) for a range of geometric ratios γ.
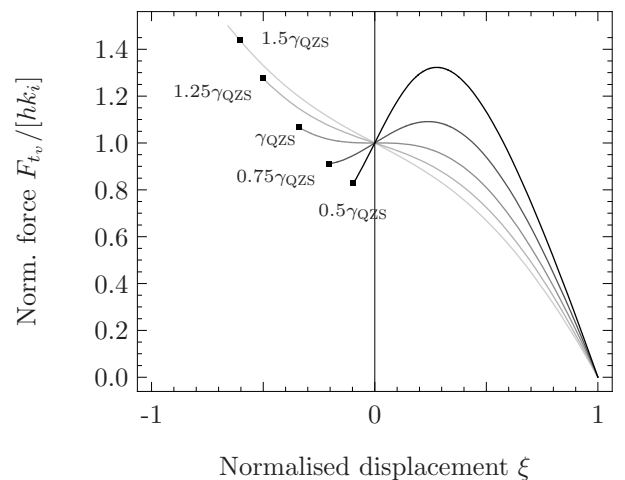
(b) Normalised vertical force characteristic of the system calculated with Eq. (8). Minimum displacements are calculated from Eq. (9); these termination points represent the limiting case of the vertical spring being compressed to zero length.

Figure 2. Vertical forces due to the inclined springs. γ_{QZS} is the value of γ for which quasi–zero stiffness is achieved at $\xi = 0$, calculated from Eq. (12).

The total vertical force produced by the system, $F_{t_v}(z)$, is calculated by combining Eq. (4) for each inclined spring with the force due to the vertical spring:

$$F_{t_v}(z) = 2F_{i_v}(z) + F_{v_v}(z). \tag{6}$$

For vertical displacements, the force due to the vertical spring is given by

$$F_{v_v}(z) = [h - x] k_v, \tag{7}$$

and the total force in the vertical direction can be nondimensionally represented by

$$\frac{F_{t_v}(z)}{hk_i} = -\xi \alpha + \alpha + 2\xi \left[\sqrt{\frac{\gamma^2 + 1}{\gamma^2 + \xi^2}} - 1 \right], \tag{8}$$

recalling that $\alpha = k_v/k_i$ is the stiffness ratio between the vertical and inclined springs. This equation is depicted in Figure 2b for a

unity stiffness ratio ($\alpha = 1$), where it can be seen that by selecting the geometric ratio γ appropriately it is possible to generate a local region of low stiffness at displacement $\xi = 0$, approaching the quasi–zero stiffness condition under ideal circumstances. The calculation for γ_{QZS}, the value of the geometric ratio γ for which quasi–zero stiffness is achieved, will be shown later in Eq. (12).

The force curves in Figure 2b terminate at a certain point in the negative displacement region, which corresponds to the maximum possible compression of the vertical spring, given by the condition $H(z_{\min}, 0) = 0$. In other words, the spring has been compressed to zero length (which would be troublesome to achieve in practice). This condition can be solved for $z_{\min}$ and subsequently normalised for the equivalent $\xi_{\min}$, which are given by

$$z_{\min} = h - H_0, \qquad \xi_{\min} = 1 - \eta\sqrt{\gamma^2 + 1}. \qquad (9)$$

VERTICAL STIFFNESSES

The vertical stiffness characteristic, K_v, of the system is calculated by differentiating the vertical force, Eq. (8), with respect to vertical displacement z:

$$K_v = -\frac{d}{dz}F_{t_v}(z), \qquad (10)$$

$$\frac{K_v}{k_i} = -2\gamma^2\sqrt{\frac{\gamma^2 + 1}{\left[\gamma^2 + \xi^2\right]^3}} + \alpha + 2. \qquad (11)$$

Graphs of the normalised vertical stiffness K_v/k_i versus normalised displacement ξ are shown in Figure 3a together with the associated horizontal stiffness (Figure 3b), which will be analysed in the next section. The parameter selection required to achieve a quasi–zero stiffness condition in the vertical direction can be found by solving Eq. (11) for $K_v = 0$ at $\xi = 0$. This results in the relation

$$\gamma_{QZS} = \frac{2}{\sqrt{\alpha^2 + 4\alpha}} \qquad (12)$$

which is used as the reference value of the geometric ratio γ for the results shown in Figures 2 and 3.

Achieving exactly quasi–zero stiffness with this spring is not feasible in practice as the stiffness characteristic becomes negative for $\gamma < \gamma_{QZS}$, as shown in Figure 3a. This is important as the geometric ratio γ will have some uncertainty in its value due to environmental conditions such as temperature and physical imperfections such as creep. The deviation of γ from γ_{QZS}, ε, can be defined by

$$\gamma = \left[1 + \varepsilon\right]\gamma_{QZS}. \qquad (13)$$

Figure 4a shows the total vertical force, $F_{t_v}(z)$, of the system for $\varepsilon \in \{-0.1, 0, 0.1\}$. It can be seen that negative values of ε (that is, a geometric ratio less than that for quasi–zero stiffness) correspond to negative stiffness at normalised displacement $\xi = 0$. A system in this condition is in a position of unstable equilibrium, and will move towards and remain at the position of stable equilibrium indicated in the figure rather than the design point at $\xi = 0$.

Figure 4b plots the stiffness at this deviated equilibrium point as ε varies; in the unstable zone, the system will move to the equilibrium point shown in Figure 4a away from $\xi = 0$. (With sufficient excitation the system will 'snap though' from one equilibrium position to another with a resulting displacement profile that is comparatively large given the excitation amplitude; this mechanism has been proposed as a useful phenomenon for energy harvesting purposes (Ramlan, Brennan, Mace, and Kovacic
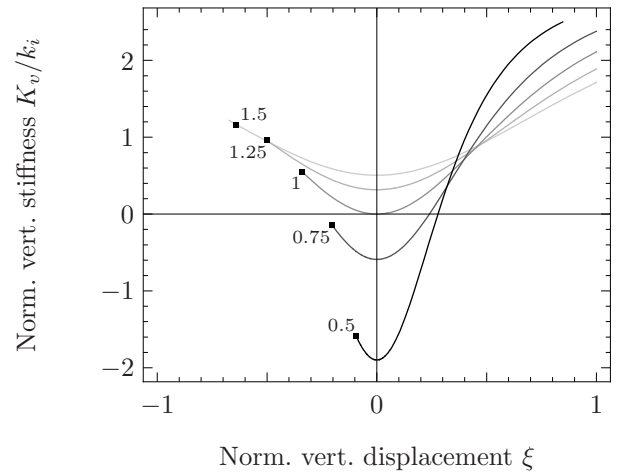
(a) Normalised vertical stiffness of the system calculated with Eq. (11).
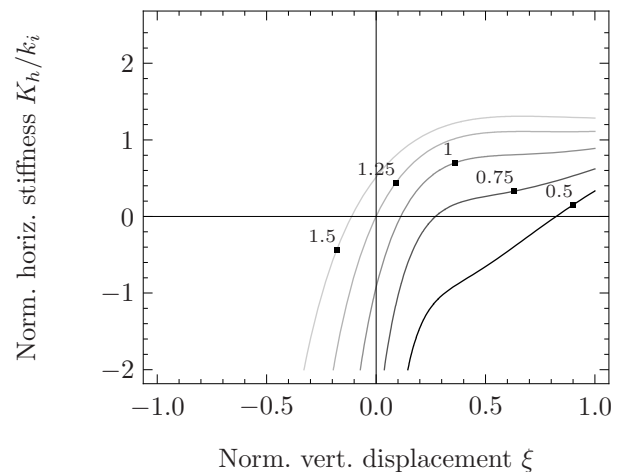
(b) Normalised horizontal stiffness of the system calculated with Eq. (19).

Figure 3. Vertical and horizontal stiffness characteristics for a range of geometric ratios γ at $\alpha = 1$. Plots are labelled with their ratio to γ_{QZS}, which is calculated for a length ratio of $\eta = 1$.

2009).) It can be seen that the stiffnesses in the stable region for $\varepsilon > 0$ are smaller than the stiffnesses in the equilibrium region for $\varepsilon < 0$. This highlights the importance of never breaching the $\varepsilon < 0$ instability condition. Therefore, a chosen value for the geometric ratio γ will approach γ_{QZS} but always be slightly greater in order to retain stability of the equilibrium position.

## HORIZONTAL STIFFNESS CHARACTERISTIC

Now that the vertical stiffness characteristics of the system have been analysed and a condition derived to achieve quasi–zero stiffness in that direction, the same approach will be taken for the horizontal behaviour.

In order to calculate the horizontal stiffness of the system, the force from the vertical spring needs to be represented in terms of both vertical and horizontal displacements. This force, aligned in the direction of the nominally-vertical spring, is
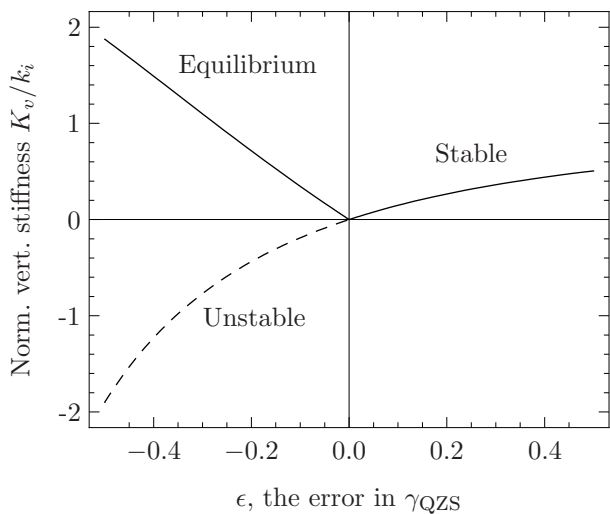
$$F_v(z, x) = \left[\eta L_0 - \sqrt{x^2 + \left[-h + z + \eta L_0\right]^2}\right]k_v, \qquad (14)$$

recalling that x is the displacement of the mass in the horizontal direction. Substituting $x = 0$ into Eq. (14) yields the previous Eq. (7). The horizontal component of this force is

$$F_{v_h}(z, x) = F_v(z, x)\frac{x}{H(z, x)}. \qquad (15)$$
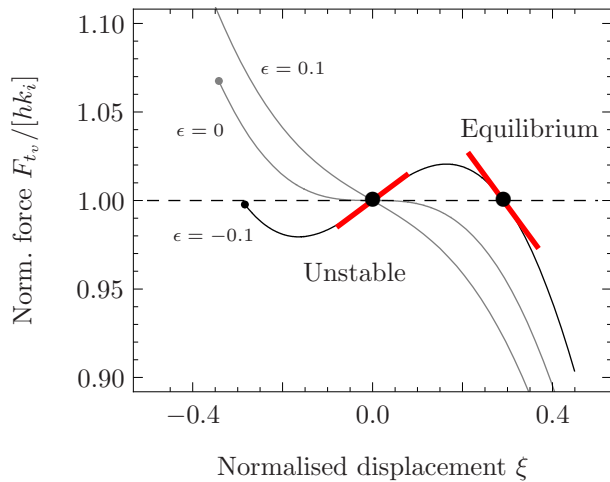
(a) The stable and unstable equilibrium points for $\varepsilon \in \{-0.1, 0, 0.1\}$. The rest position will move from the unstable point to the stable point of equilibrium.

(b) The stiffness at equilibrium as ε varies; as the stiffness becomes negative, the stiffness shown corresponds to the stable point of equilibrium shown in the figure adjacent.

Figure 4. Force and stiffness of the inclined spring system near quasi–zero stiffness, showing the effect of unstable equilibrium.

Similarly, the horizontal component of the force from the inclined spring on the left (referring to Figure 1a) is given by

$$F_{i_h}(z,x) = F_i(z,x)\frac{w+x}{L(z,x)}, \qquad (16)$$

and the horizontal component of the force from the inclined spring on the right is

$$F_{i_h}(z,x)\Big|_{\text{right}} = -F_{i_h}(z,-x). \qquad (17)$$

The stiffness characteristic in the horizontal direction, K_h, is derived in a similar fashion to the vertical stiffness. The total force in the horizontal direction is

$$F_{t_h}(z,x) = F_{i_h}(z,x) - F_{i_h}(z,-x) + F_{v_h}(z,x), \qquad (18)$$

using Eqs (15) and (16). Differentiating with respect to horizontal displacement x and evaluating at $x = 0$ gives the horizontal stiffness characteristic as the vertical displacement varies,

$$\frac{K_h}{k_i} = -2\xi^2\sqrt{\frac{\gamma^2+1}{[\gamma^2+\xi^2]^3}} + \frac{\alpha[\xi-1]}{\eta\sqrt{\gamma^2+1}+\xi-1} + 2. \qquad (19)$$

This equation has been previously graphed together with the vertical stiffness in Figure 3 on the preceding page. In these figures, it can be seen that while the vertical stiffness is zero at normalised displacement $\xi = 0$ and geometric ratio $\gamma = \gamma_{\text{QZS}}$ (which is as derived), the horizontal stiffness exhibits separate behaviour, and can even be negative (that is, unstable) for values of γ lower than around $1.25\gamma_{\text{QZS}}$.

Since the vertical stiffness and horizontal stiffness are independent, further analysis into the behaviour of the horizontal stiffness at the vertical quasi–zero stiffness condition is warranted. Substituting the quasi–zero stiffness condition of Eq. (12) into Eq. (19) at displacement $\xi = 0$, gives the normalised horizontal stiffness as a function of stiffness ratio α:

$$\frac{K_h}{k_i}\bigg|_{\text{V. QZS}} = 2 - \alpha\left[\frac{[\alpha+2]\,\eta}{\sqrt{\alpha[\alpha+4]}} - 1\right]^{-1}. \qquad (20)$$

This equation is depicted in Figure 5; it can be seen that the horizontal stiffness of the spring may be chosen by varying both the spring stiffness ratio α and the spring length ratio η. Since the length ratio η is not found in Eq. (11), the horizontal and vertical stiffnesses may be tuned independently in order to achieve quasi–zero stiffness in both simultaneously.
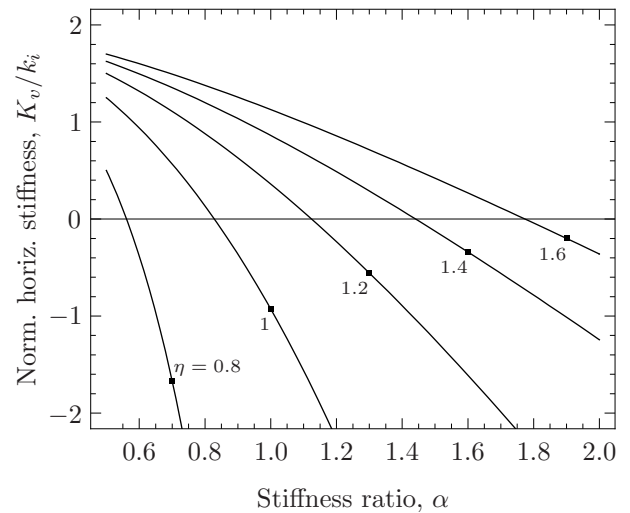

Figure 5. Horizontal stiffness characteristic at the vertical quasi–zero stiffness condition for varying stiffness ratio α and length ratio η, calculated with Eq. (20).

To obtain quasi–zero stiffness in the horizontal direction, Eq. (20) is solved at $K_h = 0$, showing a relationship between α and η when the quasi–zero stiffness condition is achieved in both the vertical and the horizontal directions.

$$\alpha_{\text{QZS}}(\eta) = 2\left[\sqrt{\eta^2+1} - 1\right], \text{ or}$$
$$\eta_{\text{QZS}}(\alpha) = \frac{1}{2}\sqrt{\alpha[\alpha+4]}. \qquad (21)$$

As a consequence, increasing η (say, in order to reduce the compression of the vertical spring) results in an increasing value of the vertical spring stiffness in order to remain at quasi–zero stiffness.

Using α_{QZS} from Eq. (21) in the stiffness equations (11) and (19) allows the stiffness characteristics of the system in the two directions to be compared when both have quasi–zero stiffness simultaneously. Considering the vertical stiffnesses first in Figure 6a, it can be seen that increasing the length ratio η increases the vertical stiffness gradient, which is an important parameter to be kept small in order to mitigate possible nonlinear dynamic effects that may arise due to a large rate of change of stiffness over displacement.

Figure 6b illustrates that the quasi–zero stiffness condition is always marginally unstable in the horizontal direction since negative displacement will result in negative stiffness. In practice this requires that the system be tuned slightly away from the quasi–zero stiffness condition in the horizontal direction after accommodating for the maximum disturbance displacement of the isolator. It is possible to do this without compromising the quasi–zero stiffness condition in the vertical direction because the spring length ratio η does not affect the vertical stiffness.

As an example, Figure 7 shows the horizontal stiffness for a stiffness ratio detuned by five percent below that required for quasi–zero stiffness (that is, $\alpha = 0.95\alpha_{QZS}$). In comparison with Figure 6b, the spring has a stable displacement range of approximately $\xi = \pm0.025$. Provided that the spring length ratio η is large enough, the horizontal stiffness at $\xi = 0$ is still significantly reduced.

Therefore, there is a direct compromise between the nonlinearity of the stiffness in the vertical direction (which increases with η) and the amount of stiffness reduction in the horizontal direction (which decreases with η).
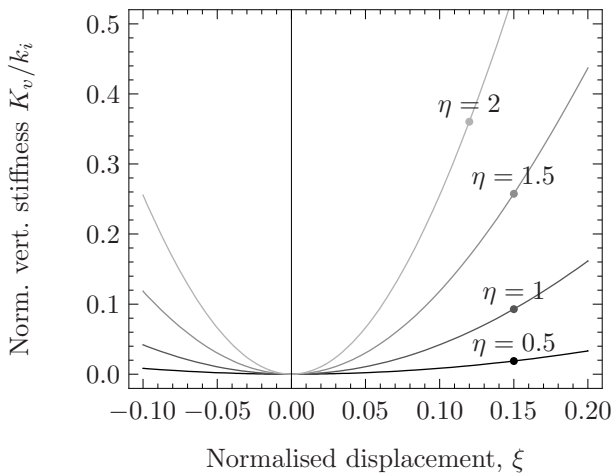
(a) Normalised vertical stiffness of the system.
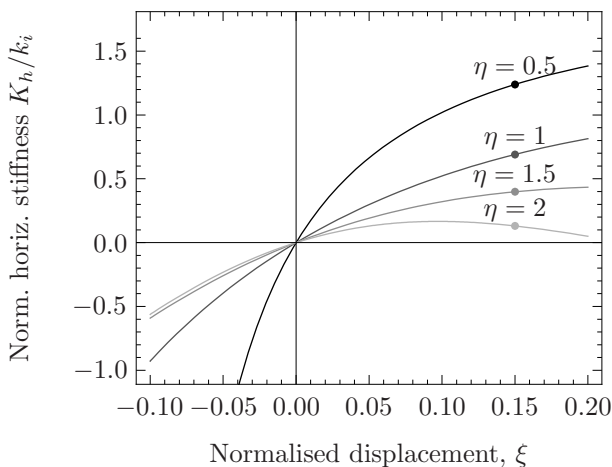
(b) Normalised horizontal stiffness of the system; negative displacement will result in negative stiffness.

Figure 6. Vertical and horizontal stiffness characteristics at quasi–zero stiffness in both directions, for a range of spring length ratios, η.

SPRING COMPRESSION

One factor that has not been addressed with this particular design is the amount of spring compression required at the equilibrium position of quasi–zero stiffness. The total allowable
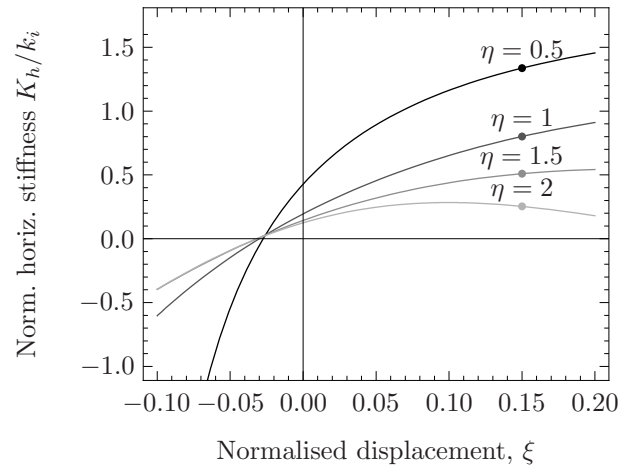

Figure 7. Normalised horizontal stiffness of the system at $\alpha = 0.95\alpha_{QZS}$ in order to obtain a small range of displacement around $\xi = 0$ with positive stiffness (compare with Figure 6b which has negative stiffness for $\xi < 0$). The vertical quasi–zero stiffness condition is unaffected.

compression will be limited by the shape and properties of the springs themselves. By adjusting the design parameters of the inclined spring system, the amount of compression in each spring at equilibrium can be selected.

The amount of spring compression can be analysed with a metric here called the 'compression ratio' related to the uncompressed spring length. For the inclined and vertical springs, respectively, the compression ratios C_i and C_i are given by

$$C_i = 1 - \frac{L(z,x)}{L_0}, \quad C_v = 1 - \frac{H(z,x)}{H_0}. \quad (22)$$

This metric for the compression ratio was chosen to be zero for a spring in its uncompressed position and unity if it is compressed to its full length (which is the theoretical limit for springs in compression).

The compression ratios were evaluated at the quasi–zero stiffness condition in both directions; that is, $(z,x) = (0,0)$, $\gamma = \gamma_{QZS}$, and $\eta = \eta_{QZS}$ (see Eqs (12) and (21)), yielding

$$C_i\Big|_{QZS} = \frac{\alpha}{\alpha + 2}, \quad C_v\Big|_{QZS} = \frac{2}{\alpha + 2}. \quad (23)$$

The compression ratios of the vertical and inclined springs at quasi–zero stiffness are shown in Figure 8 as functions of varying spring stiffness ratio α. (Recall that quasi–zero stiffness is achieved by adjusting η for each specified value of α with the relationship shown in Eq. (21).) These results show that a large compression (greater than fifty percent) in at least one of the springs is required to achieve quasi–zero stiffness.

THE GENERAL APPLICABILITY OF THE INCLINED SPRINGS SYSTEM

In order to adapt this system to withstand time-varying load conditions, both the anchor positions of the inclined and the vertical springs must be adjusted in order to tune for, first, the required load bearing, and second, the amount of negative stiffness required to achieve quasi–zero stiffness in the vertical direction.

Dynamically changing the system for quasi–zero stiffness in the horizontal direction requires that either the uncompressed
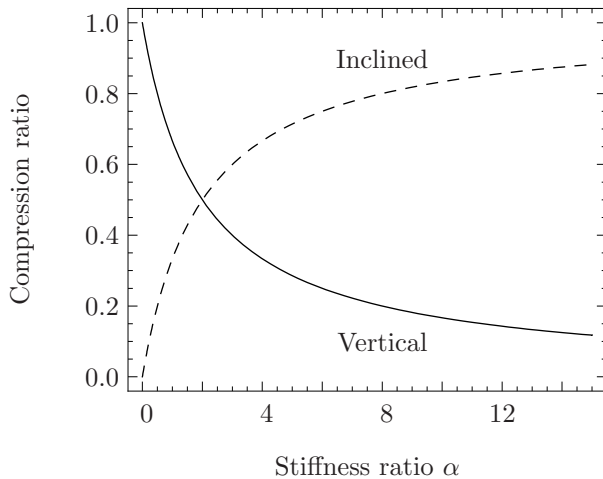
Figure 8. Compression relationship of the springs for a range of spring stiffness ratios, at quasi–zero stiffness both horizontally and vertically. A compression of 100% implies a change in displacement of the entire spring length, which is difficult to realise in practice.

spring lengths or the spring stiffnesses be adjustable during operation. Since the deflection properties of the spring cannot be adjusted, a time-varying stiffness is required. This could be achieved, for example, with magnetorhealogical fluid springs; others have achieved such effects using leaf springs in a four-bar linkage (Choi, Hong, Lee, Kang, and Kim 2011).

Note that the principles discussed for horizontal stiffness can be extended to a three-dimensional system, most easily with a rotationally-symmetric structure with horizontally aligned springs in each plane.

CONCLUSION

This paper has analysed the horizontal stiffness characteristics of a common quasi–zero stiffness arrangement that uses linear mechanical springs. This system has been analysed extensively in the literature with respect to its vertical stiffness properties and its suitability for vibration isolation; this work has shown that with correctly tuned spring stiffnesses, low horizontal stiffness can be achieved simultaneously with low vertical stiffness. However, the tuning required to maintain quasi–zero stiffness for this spring arrangement is difficult to achieve in practice.

REFERENCES

Alabuzhev, P., A. Gritchin, L. Kim, G. Migirenko, V. Chon, and P. Stepanov (1989). *Vibration Protecting and Measuring Systems with Quasi-Zero Stiffness*. Ed. by E. Rivin. Applications of Vibration. Hemisphere Publishing Corporation. ISBN: 0-89116-811-7.

Carrella, A., M. J. Brennan, and T. P. Waters (Apr. 2007). "Static analysis of a passive vibration isolator with quasi-zero-stiffness characteristic". *Journal of Sound and Vibration* 301.3–5, pp. 678–689. DOI: 10.1016/j.jsv.2006.10.011.

Carrella, A., M. J. Brennan, I. Kovacic, and T. P. Waters (May 2009). "On the force transmissibility of a vibration isolator with quasi-zero-stiffness". *Journal of Sound and Vibration* 322.4–5, pp. 707–717. DOI: 10.1016/j.jsv.2008.11.034.

Cella, G., V. Sannibale, R. DeSalvo, S. Marka, and A. Takamori (2005). "Monolithic geometric anti-spring blades". *Nuclear Instruments and Methods in Physics Research Section A: Accelerators, Spectrometers, Detectors and Associated Equipment* 540.2-3, pp. 502–519. DOI: 10.1016/j.nima.2004.10.042.

Choi, J., S. Hong, W. Lee, S. Kang, and M. Kim (Apr. 2011). "A Robot Joint With Variable Stiffness Using Leaf Springs". *IEEE Transactions on Robotics* 27.2, pp. 229–238. DOI: 10.1109/TRO.2010.2100450.

Kovacic, I., M. J. Brennan, and T. P. Waters (2008). "A study of a nonlinear vibration isolator with a quasi-zero stiffness characteristic". *Journal of Sound and Vibration* 315.3, pp. 700–711. DOI: 10.1016/j.jsv.2007.12.019.

Lee, C.-M., V. N. Goverdovskiy, and A. I. Temnikov (May 2007). "Design of springs with "negative" stiffness to improve vehicle driver vibration isolation". *Journal of Sound and Vibration* 302.4–5, pp. 865–874. DOI: 10.1016/j.jsv.2006.12.024.

Molyneux, W. G. (1957). *Supports for vibration isolation*. ARC/CP-322. Aeronautical Research Council, Great Britain. URL: http://nsdl.org/resource/2200/20061003060308472T.

Ramlan, R., M. Brennan, B. Mace, and I. Kovacic (Mar. 2009). "Potential benefits of a non-linear stiffness in an energy harvesting device". *Nonlinear Dynamics* 59.4, pp. 545–558. DOI: 10.1007/s11071-009-9561-5.

Robertson, W. S., M. R. F. Kidner, B. S. Cazzolato, and A. C. Zander (2009). "Theoretical design parameters for a quasi-zero stiffness magnetic spring for vibration isolation". *Journal of Sound and Vibration* 326.1–2, pp. 88–103. DOI: 10.1016/j.jsv.2009.04.015.

Tarnai, T. (Mar. 2003). "Zero stiffness elastic structures". *International Journal of Mechanical Sciences* 45.3, pp. 425–431. DOI: 10.1016/S0020-7403(03)00063-8.

Xing, J. T., Y. P. Xiong, and W. G. Price (2005). "Passive-active vibration isolation systems to produce zero or infinite dynamic modulus: Theoretical and conceptual design strategies". *Journal of Sound and Vibration* 286.3, pp. 615–636. DOI: 10.1016/j.jsv.2004.10.018.

Xu, D., Q. Yu, J. Zhou, and S. Bishop (July 2013). "Theoretical and experimental analyses of a nonlinear magnetic vibration isolator with quasi-zero-stiffness characteristic". *Journal of Sound and Vibration* 332.14, pp. 3377–3389. DOI: 10.1016/j.jsv.2013.01.034.

Zhou, N. and K. Liu (2010). "A tunable high-static-low-dynamic stiffness vibration isolator". *Journal of Sound and Vibration* 329.9, pp. 1254–1273. DOI: 10.1016/j.jsv.2009.11.001.

Zhu, T., B. Cazzolato, W. Robertson, and A. Zander (2011). "The development of a 6 degree of freedom quasi-zero stiffness maglev vibration isolator with adaptive-passive load support". *15th International Conference on Mechatronics Technology*. URL: http://hdl.handle.net/2440/72548.